TISSUE ENGINEERING: Part A
Volume 26, Numbers 13 and 14, 2020

DOI: 10.1089/ten.tea.2020.0033

termis
Tissue Engineering
& Regenerative Medicine
International Society

SPECIAL ISSUE ON WOMEN'S HEALTH

Transcriptomic Analysis of Human Mesenchymal Stem Cell Therapy in Incontinent Rat Injured Urethra

Zhina Sadeghi, MD,[1] Jonathan D. Kenyon, PhD,[2] Brian Richardson, PhD,[3]
Ahmad O. Khalifa, MD,[4,5] Michael Cartwright, PhD,[6] Britt Conroy, MD,[7] Arnold Caplan, PhD,[8]
Mark J. Cameron, PhD,[9] and Adonis Hijaz, MD[10]

Periurethral human mesenchymal stem cell (hMSC) injections are associated with functional improvement in animal models of postpartum stress urinary incontinence (SUI). However, limited data exist on the role of hMSCs in modulating gene expression in tissue repair after urethral injury. To this end, we quantified temporal gene expression modulation in hMSCs, and in injured rat urethral tissue, using RNA-seq in an animal model of SUI, over a 3-day period following urethral injury, and local hMSC injection.

We injected PKH fluorescent-labeled hMSC into the periurethral space of rats following a 4 h vaginal distention (VD) (three rats per time point). Control rats underwent VD injury only, and all animals were euthanized at 12, 24, 36, 72 h postinjury. Rat urethral and vaginal tissues were frozen and sectioned. Fluorescent labeled hMSCs were distinguished from adjacent, unlabeled rat urethral tissue. RNA was prepared from hMSCs and urethral tissue obtained by laser dissection of frozen tissue sections and sequenced on an Illumina HiSeq 2500. Differentially expressed genes (DEGs) over 72 h were evaluated using a two-group *t*-test ($p < 0.05$).

Our transcriptional analyses identified candidate genes involved in tissue injury that were broadly sorted by injury and exposure to hMSC throughout the first 72 h of acute phase of injury. DEGs in treated urethra, compared with untreated urethra, were functionally associated with tissue repair, angiogenesis, neurogenesis, and oxidative stress suppression. DEGs included a variety of cytokines, extracellular matrix stabilization and regeneration genes, cytokine signaling modification, cell cycle regulation, muscle differentiation, and stabilization. Moreover, our results revealed DEG changes in hMSCs (PKH-labeled) harvested from injured urethra. The expressions are related to DNA damage repair, transcription activation, stem cell regulation, cell survival, apoptosis, self-renewal, cell proliferation, migration, and injury response.

Keywords: RNA sequencing, host tissue healing, urinary incontinence, mesenchymal stem cell therapy, vaginal birth trauma, acute phase of injury

Impact Statement

Stress urinary incontinence (SUI) affects nearly half of women over 40, resulting in reduced quality of life and increased health care cost. Development of SUI is multifactorial and strongly associated with vaginal delivery. While stem cell therapy in animal models of SUI and limited preliminary clinical trials demonstrate functional improvement of SUI, the role of stem cell therapy in modulating tissue repair is unclear impeding advanced clinical trials. Our work provides a new understanding of the transcriptional mechanisms with which human mesenchymal stem cells improve acute injury repair thus guiding the development of cell-based therapies for women with nonacute established SUI.

[1]University Hospitals Cleveland Medical Center, Urology Institute, Cleveland, Ohio, USA.
[2]Biology Department, Skeletal Research Center, Case Western Reserve University, Cleveland, Ohio, USA.
[3]Department of Population and Quantitative Health Sciences, Case Western Reserve University, Cleveland, Ohio, USA.
[4]University Hospitals Cleveland Medical Center, Urology Institute, Cleveland, Ohio, USA.
[5]Menoufia University Faculty of Medicine, Urology, Shebin El-Kom, Egypt.
[6]Department of Population and Quantitative Health Sciences, Case Western Reserve University, Cleveland, Ohio, USA.
[7]University Hospitals Cleveland Medical Center, Urology Institute, Cleveland, Ohio, USA.
[8]Biology Department, Skeletal Research Center, Case Western Reserve University, Cleveland, Ohio, USA.
[9]Department of Population and Quantitative Health Sciences, Case Western Reserve University, Cleveland, Ohio, USA.
[10]University Hospitals Cleveland Medical Center, Urology Institute, Cleveland, Ohio, USA.

Introduction

URINARY INCONTINENCE (UI) is a highly prevalent, socially debilitating crosscultural and costly public health problem mostly affecting females. Stress urinary incontinence (SUI) is the most common type of UI in pregnant and postpartum women.[1] In North America, the prevalence of stress UI during pregnancy, and after delivery ranges from 18% to 75%.[2,3]

Vaginal birth trauma in early adulthood is a sentinel event in a woman's urinary continence trajectory inducing mechanical and ischemic damage to female pelvic organs, including the distal urinary and gastrointestinal tract, pelvic floor muscles, connective tissue, nerves, and vasculature leading to pelvic floor dysfunction and morbidity, notably UI. Vaginal birth-induced pelvic floor muscle and nerve avulsion, connective tissue rupture, and nerve compression are strongly implicated in the pathogenesis, development, and progression of UI.[4–7] Failure to resolve pelvic floor injury following vaginal birth trauma/injury leads to persistent postpartum SUI often worsening with advancing age.[3]

The most commonly performed surgical repair techniques for SUI are implantation of synthetic mesh midurethral slings in women. However, surgery is incapable of biologic restoration of the pelvic floor.[8] Numerous recent, serious surgical complications associated with synthetic mesh implants in women undergoing pelvic floor repair have garnered national attention prompting the Food and Drug Administration (FDA) to ban transvaginal synthetic mesh.[8,9]

Mesenchymal stem cells (MSCs)[10] are promising as an effective, minimally invasive restorative treatment for SUI in animal models[11] and early clinical trials.[12] We previously demonstrated periurethral injection of human mesenchymal stem cells (hMSCs) following vaginal injury, in a rat model of postpartum SUI, is therapeutically beneficial as measured by increased urinary leak-point pressure compared with untreated control animals.[13]

The mechanisms underlying improved continence after hMSC treatment remains elusive. Mounting evidence suggests that hMSCs applied to injuries improve tissue regeneration through paracrine factor secretion involving cytoprotection, neovascularization, anti-inflammation, antifibrosis, proliferation, differentiation, migration, and metabolism.[14] Proposed cytoprotection mechanisms include antiapoptotic, antinecrosis effects through the secretion of insulin-like growth factor (IGF-1),[15] epidermal growth factor (EGF),[15] and vascular endothelial growth factor (VEGF).[15] Promoting neovasculogenesis has also been suggested to occur through VEGF secretion,[16] HGF,[16] TGF-β,[17] and IGF-1.[16] Suppressing inflammation and improving healing postischemic/reperfusion injury is known to occur through interferon-γ, TNF-α,[18,19] and CCL2.[20] hMSCs suppress fibrosis through extracellular matrix (ECM) remodeling and increased collagen expression.[21] hMSCs stimulate proliferation, differentiation, and migration of injured host tissue cells, resulting in increased endogenous regeneration through factors, including HGF,[22] FGF2, and PDGF.[23]

To explore temporal transcriptional changes of injured urethral tissue post-MSC treatment, and hMSCs applied to the injured urethra, we injected hMSCs into urethral tissue of a rat SUI injury model of vaginal distention (VD). We then determined the transcriptome and differentially expressed genes (DEGs) by RNA-seq of laser-dissected injured rat urethral tissue and PKH-labeled hMSCs at 12, 24, 36, and 72 h posttrauma/intervention. These samples were then compared with expression profiles of tissue obtained from untreated injured urethral tissue. We report the most significant DEGs longitudinally, between hMSC treated and untreated urethral tissue, and within injury injected hMSC.

Materials and Methods

Human mesenchymal stem cell preparation

Human hMSCs were isolated from bone marrow aspirated from the iliac crest of a49-year-old, healthy female human donor, after informed consent was obtained, under a protocol approved by the Institutional Review Board (IRB) at University Hospitals of Cleveland (IRB 09-90-195, approved December 3, 2012), according to previously published methods.[24] We cultured the hMSCs in low-glucose Dulbecco's Modified Eagle Medium +10% fetal bovine serum (MSC screened lot) and harvested the fourth passage for cell administration. hMSCs were labeled using the PKH Red Fluorescent Cell Linker Kit (Sigma-Aldrich, Merck KGaA, Darmstadt, Germany). PKH incorporates the reporter molecules into the cell membrane, and labeled cells retain both biological and proliferative activity.[25]

Animal model, cell administration, tissue preparation, and laser capturing

VD injury was carried out as previously described.[13] Sprague-Dawley Rats ($n=24$, weight: 240–260 g) underwent standardized 4 h VD. The rat vagina was accommodated with metal dilators, followed by placement of a modified #10F Foley's catheter, inflated with ~3 cc water. Immediately after VD, 12 rats were treated with 1×10^6 PKH-labeled hMSCs through the anterior wall of the vagina and into the periurethral space. The remaining 12 rats were treated with saline injection (untreated control). Rats ($n=3$/group) in the treated and untreated groups were euthanized at 12-, 24-, 36-, and 72-h time points. Rats were anesthetized by intraperitoneal urethane, for tissue harvest then euthanized. The urethral/periurethral tissue, adjacent anterior vaginal wall, and injected hMSCs were harvested and embedded in O.C.T. Compound (Tissue Plus, Scigen, CA), for immediate freezing. This maintained an intact tissue plane between urethra and vagina during sectioning. The tissues were placed in O.C.T. embedding medium, immediately solidified on liquid nitrogen, and then stored at −80°C. Cryoembedded urethral tissues were sectioned and stained with DAPI (4′,6-diamidino-2-phenylindole) fluorescent DNA stain. Sections containing PKH-positive cells were identified, and stained cells were captured using a Leica LMD6 laser microdissection microscope; Figure 1. Urethral tissue adjacent to the captured hMSC area and devoid of stained hMSC was also laser captured as a separate sample. In untreated (VD only) group, urethral tissues were captured starting from midurethral/vaginal plane. For each animal urethral block, 40–45 tissue sections were captured, to obtain sufficient RNA.

RNA sequencing

Laser-capture microdissection samples were preserved in RNAlater (Invitrogen) with RNA isolation performed using

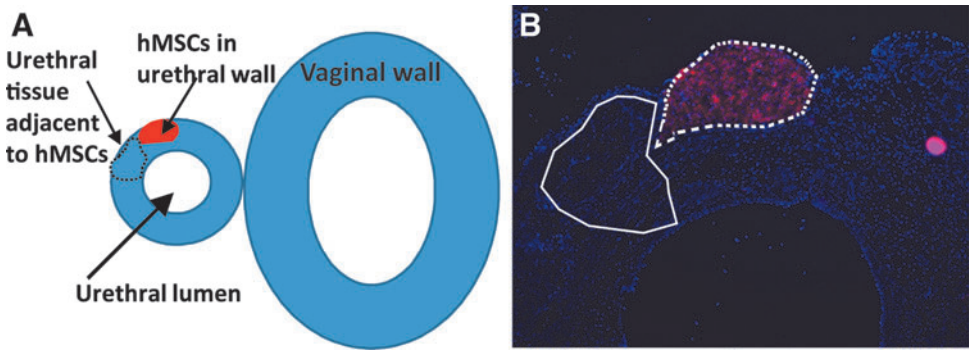

FIG. 1. **(A)** Overview of the urethra and vaginal tissue and location of the PKH-labeled hMSCs, and urethral tissue adjacent to hMSCs to be captured. **(B)** PKH-labeled hMSC (*red*) observed in a cryopreserved urethral tissue section overlain with sections to be removed by laser dissection. hMSC, human mesenchymal stem cell.

the Qiagen RNEasy Micro Kits. RNA quality evaluation and quantification was performed on Advanced Analytical's Fragment Analyzer using the High Sense RNA Kits. The amount of RNA extracted was greater than 100 pg/sample and had a mean RQN quality score of 8.4 with a minimum value of 4.4. Total RNA was normalized to 100 pg before oligo-dT capture and cDNA synthesis with the TaKaRa's SMART-Seq v4 Low Input Kits. The resulting cDNA was assessed on the Fragment Analyzer with the High Sense Large Fragment Kit and quantified using a Life Technologies' Qubit 3.0 fluorometer. Libraries were generated using the Illumina's Nextera XT DNA Library Prep Kit. mRNA sequencing was performed with an Illumina HiSeq 2500 using a Rapid Run v2, 100 base pair, Paired-End design, resulting in >15 million paired-end reads per sample.

RNA sequencing analysis

Raw demultiplexed fastq paired-end read files were trimmed of adapters and filtered using the program skewer[26] to discard reads with an average phred quality score of less than 30, or a length shorter than 36. Trimmed reads were then aligned using the HISAT2 aligner to the *Rattus norvegicus* NCBI reference genome assembly version Rnor_6.0 and sorted using SAM tools.[27,28] Aligned reads were counted, and assigned, to gene metafeatures using the program featureCounts, as part of the Subread package.[29] These count files were imported into the R programming language, and were assessed for quality control, normalized, and analyzed using the edgeR Bioconductor library for differential gene expression testing, and the GSVA library for gene set variation analysis.[30,31] The filtered count values used in the analysis can be found in Supplementary Tables S1 and S2 for the Rat Urethra and Human MSC samples, respectively. To assess the overall relationship between the rat urethra samples and treatment and/or time points following VD, we performed principal component analysis (PCA), an analytical method converting correlated datasets into a set of values of linearly uncorrelated variables (principal components), the first of which contains the largest possible variance (dimension1). A p-value of 0.05 was used as the defined criteria of significance/DEGs, as well as the genes used to create the PCA. For the hMSC-captured time-based PCA, the PCA method was run on the log2 counts per million (CPM) transformed count matrix for genes with a p-value <0.05 in any one of the comparisons between two time points. For the rat urethra treated sample PCA, the comparison was done with each group being compared as a whole (time points were combined), such that any gene with $p \leq 0.05$ in the treated versus untreated comparisons were included. The first two principal components were then graphed.

To demonstrate urethral tissue dynamic gene expression modulation, we focused on the DEGs ranked highest by p-value between hMSC treated injured urethra compared with untreated injured urethra. We sought to determine how gene expression in urethral tissue changed over time in treated versus untreated urethra. Thus, we quantified the number of DEGs between treated and untreated urethral tissue at each time point. Hierarchical clustering was performed using complete-linkage clustering and Euclidean distance for either the rows (genes) or columns (samples) shown in the heat maps. DEGs are color scaled using z-scores of the log2 CPM of each gene so that different clusters of samples and their gene expression can be interpreted relative to each other.

To characterize the differences between hMSCs captured from hMSC treated urethral tissue at each time point (12 vs. 24 h, 24 vs. 36 h, 36 vs. 72 h), in addition to comparing first and last time points (12 vs. 72 h) after injury, we ranked DEGs by sum total fold change, across time, by magnitude difference, and determined the top 50 most DEGs observed between captured hMSCs from pairs of consecutive time points (12 vs. 24 h, 24 vs. 36 h, 36 vs. 72 h) in addition to comparing first and last time points (12 vs. 72 h) postinjury.

Results

Transcriptional analysis of captured hMSCs, and hMSC treated versus untreated injured urethra, during acute phase of injury

The number of DEGs, determined by low-input RNA-seq (mRNA) in hMSC treated versus untreated injured rat urethra at the four study time points (12, 24, 36, and 72 h) are presented in Table 1. The number of DEGs was significantly different ($p \leq 0.05$) across the 4 study time points at 12 ($n = 626$), 24 ($n = 1260$), 36 ($n = 1260$), and 72 ($n = 975$) h after injury, and at 72 h compared with 12 h ($n = 661$) postinjury. The number of statistically significant DEGs were lowest at 12 h ($n = 636$), peaked at 24 h ($n = 1260$) and 36 h, then decreased to 975 at 72 h. When comparing hMSC DEGs harvested from treated urethra between each study time point (12, 24, 36, and 72 h), differences were significant at 24 versus 12 h ($n = 368$), 36 versus 24 h ($n = 169$), 72 versus 24 h ($n = 200$), with the largest magnitude of difference at 72 versus 12 h ($n = 382$).

Table 1. Number of Significant DEGs ($p \leq 0.05$) in Each Time Point

Comparison group	*No. of DEGs with $p \leq 0.05$*
MSC treated vs. untreated urethra 12 h	626
MSC treated vs. untreated urethra 24 h	1260
MSC treated vs. untreated urethra 36 h	1260
MSC treated vs. untreated urethra 72 h	975
MSC treated urethra 72 vs. 12 h	661
MSC harvested from 24 vs. 12 h treated urethra	368
MSC harvested from 36 vs. 24 h treated urethra	169
MSC harvested from 72 vs. 24 h treated urethra	200
MSC harvested from 72 vs. 12 h treated urethra	382

DEG, differentially expressed gene; MSC, mesenchymal stem cell.

The results of the PCA of treated and untreated laser-captured rat urethra that assessed the relationship between rat urethra samples and treatment and/or time points following VD/injury and the dataset dimensions that most explain the variance in significantly differential gene expression (time point contrasts between hMSC treated and untreated injured rat urethra) are depicted in Figure 2A. For the hMSC treated versus untreated injured rat urethra PCA, dimension1 explained 60.56% of the variance and dimension2 explained 6.52% or generally by time point and treatment group in each dimension, respectively (Fig. 2A). PCA also showed the time point contrast between hMSCs captured from injured urethra at different time points following injury. For the hMSC PCA, dimension1 explained 39.8% of the variance and dimension2 explained 11.53% or generally by time point in each dimension (Fig. 2B). These PCA results provide a relational overview of the longitudinal impact of hMSC in injured rat urethra to set the stage for further gene-level analyses in that DEG are more significantly influenced over time in our model than at a particular time point comparison.

MSC injection induces time-dependent transcriptional changes in urethral tissue following injury

We quantified the number of DEGs between treated and untreated urethral tissue at 12, 24, 36, and 72 h postinjury, where 23% of the DEGs were significant ($p < 0.05$) (Fig. 3A). We also calculated the number of the DEGs overlapping between pairs of time points; Figure 3B. This analysis was performed to determine the extent of shared DEGs between paired time points. These persistent DEGs in between time points may indicate key modified genes altered by hMSC in urethra during acute phase of injury (Fig. 3B). *CXCL1* and *SLC39a14* were the only two genes persistently differentially expressed between hMSC treatment and untreated injured urethras at all times. Our observations of *CSCL1* suggest that expression of a key neutrophil recruitment cytokine[32] was delayed in treated urethral tissue. Additionally, gene expression of *SLC39a14* is associated with exposure to an inflammatory environment.[33] Altogether, the muted expression of *SLC39a14* and delayed expression of *CXCL1* in hMSC treated urethral tissue is an indication of a milder microenvironmental response.

To compare and contrast the gene expression differences between treated and untreated urethral tissue, we ranked DEGs by sum total fold change across time by magnitude difference and determined the top 50 most DEGs observed between these two groups. We hierarchically clustered these DEGs and showed gene expression as a heat map (Fig. 4). We observed time-dependent up- and downregulation of gene expression at all times post VD.

We additionally ranked DEGs between treated and untreated urethra persistently differentially expressed at all study times by magnitude and summarized them in a heat map. The 50 most DEGs between hMSC treated and untreated urethra are depicted in Figure 5. Interestingly, these include genes involved in wound healing, including ECM stabilization and regeneration, cytokine signaling, cell cycle regulation, muscle differentiation and stabilization, angiogenesis and vasoprotection, neurogenesis and neuroprotection, and oxidative stress modification.

Comparing between treated injured urethra, and untreated injured urethra, we observed increased expression of *Eln* and *Afap1* (at 12 h); *Csrp3*, *Pdgfc*, and *Ttn* (at 24 h); *Ecm1* (at 36 h); and *Flt1*, *Slc39a14*, and *Cxcl1* (at 72 h). *Bcat1* significantly decreased at 72 h in hMSC treated urethra. This may suggest overall accelerated wound healing in first 72-h postinjury in hMSC treated urethra (Table 2).

MSC treated injured urethra demonstrates significant alteration in genes involved in angiogenesis and vasoprotection. This includes increased expression of *Egfl7* and *Zeb1* (at 12 h); *Pros1* (at 36 h); and *Cxcl1* (at 72 h) and decreased expression of *Traf6* (at 12 h) and *Angptl2* (at 24 h) in hMSC treated urethra. This suggests that hMSC treatment induces enhanced angiogenesis and vasoprotection in injured urethral tissue (Table 2).

Additionally, we detected genes involved in neuromuscular signaling, including *Acsl1* (at 12 h), *Atp2a1* (at 24 h), and *Agrn* (at 36 h), with increased expression in hMSC treated urethra. While other genes involved in neuroregeneration, including *Cd83* and *Gfra2* increased expression at 72 h. Whereas *Nfil3*, involved in neuroprotection against inflammation, decreased at 36 h. Potentially this is evidence for neurosignaling, neural degeneration, and regeneration in injured urethral tissue alteration by hMSC therapy; (Table 2).

Interestingly, our result demonstrates increased antioxidative stress gene expression, including *Atp2a1* (at 24 h), *Hmox1* (at 36 h), and *Adcy5* and *Nos3* (at 72 h) in hMSC treated injured urethral tissue. These genes have been shown to mitigate damage induced by reactive oxygen species. hMSC treatment seems to induce a protective oxidative stress response in injured adjacent urethral tissue (Table 2).

Locally injected hMSC captured from injured urethral tissue demonstrate time-dependent transcriptional changes

We first filtered DEGs in laser-captured hMSCs with a nominal *p*-value of 0.05, in at least one comparison, and then ranked genes by the absolute sum logFC across all

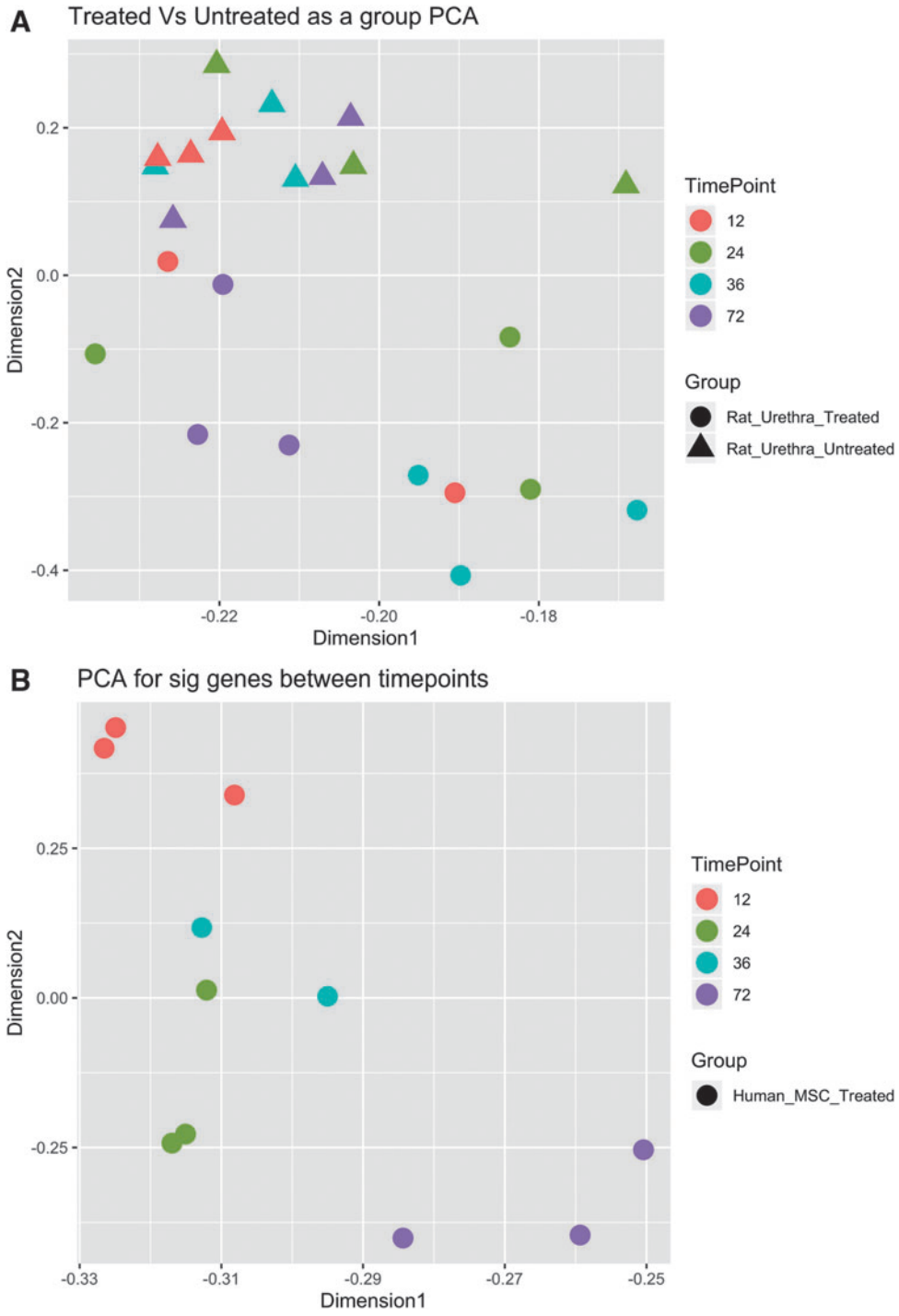

FIG. 2. PCA data: **(A)** hMSC treated and untreated laser-captured rat urethra PCA, **(B)** Laser-captured hMSC from the rat urethra PCA. $p \leq 0.05$. PCA, principal component analysis.

comparisons (12 vs. 24 h, 24 vs. 36 h, 36 vs. 72 h, and 12 vs. 72 h) (Fig. 6). We then displayed these hMSC DEGs by hierarchical clustering. The strongest cumulative differences (negative or positive) across time are shown in Figure 7. DEGs in tissue-captured hMSCs compared across sequential time points and between 12 versus 72 h demonstrate dynamic changes in hMSC gene expression over time (Table 3). Expression of genes involved in wound healing, DNA damage repair, cell fate regulation, cell survival, and apoptosis regulation increased between consecutive time points. These genes include *DDX3X*, *GPC3*, *MAP2K6*, *MAPKAPK5m* and *ZNF423* (between 12 and 24 h); *PIK3C2B* and *TEX10* (between 24 and 36 h); *DAPK2* and *NEO1* (between 36 and 72 h); and *FZD4*, *MAP2K6*, *MAP3K1*, *MYH1*, *P4HA1*, and *ZNF423* (between 12 and 72 h). A comparison of tissue-captured hMSC DEGs between consecutive time points also identified genes necessary for angiogenesis, vasoprotection, neurogenesis, and neuroprotection. Increase expression was observed in *HIF1A* and *KCNJ9* (comparing 24 to 36 h); *FGF9* and *PAQR9* (comparing 36 with 72 h); *MEF2C*, *P4HA1*, *RAB11FIP2*, and *PAQR9* (between 12 and 72 h). *KCNA1*, *NEFM*, and *STMN2* (between

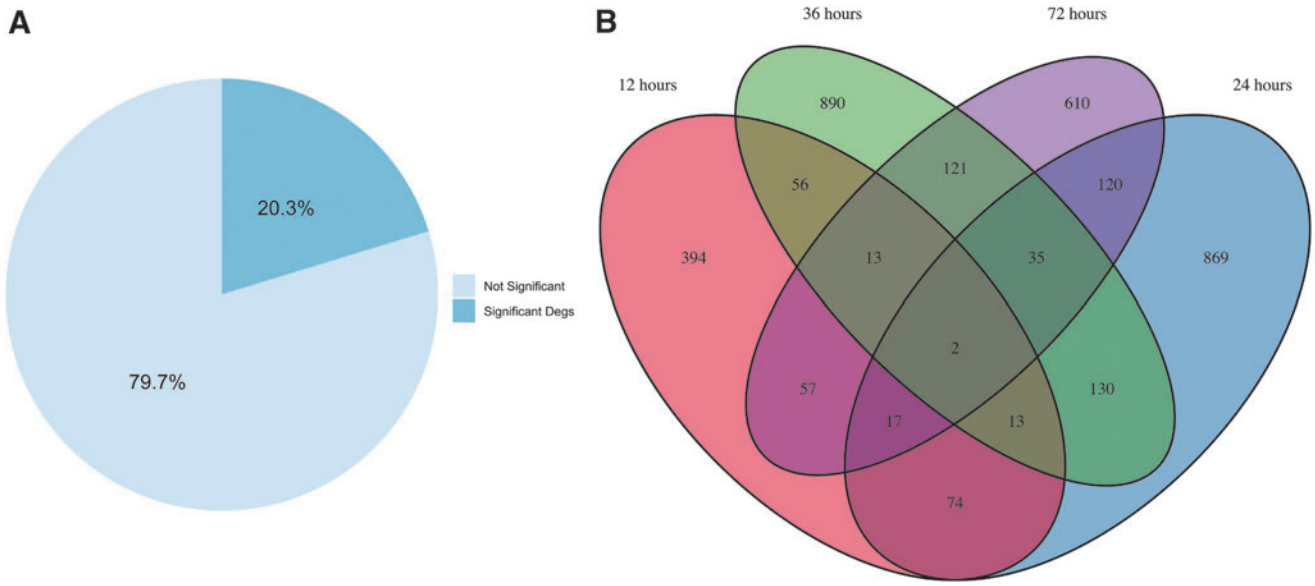

FIG. 3. **(A)** Diagram showing the overall percentage of significant ($p \leq 0.05$) and nonsignificant DEGs between hMSC treated urethra and untreated urethra considering all the DEGs at all the time points (12, 24, 36, and 72 h). **(B)** Venn diagram of the significant DEGs in hMSC treated injured urethra compared with untreated injured urethra over time with the number of overlapped DEGs between time points noted. DEG, differentially expressed gene.

24 to 36 h), and *HOXB7m* and *KCNJ9* (comparing 36 and 72 h) decreased in expression (Fig. 7). These data indicate that gene expression of therapeutically applied hMSCs is altered by injured tissue microenvironment exposure. Taken together, with the changes in urethral expression with and without hMSC treatment our data suggest urethral tissue and hMSC crosstalk.

Discussion

Although evidence demonstrates that hMSCs modulate injured host tissue response and regeneration through a variety of paracrine factors,[34–38] to date no study exists that has explored dynamic gene expression modulation within xenograft hMSCs, and urethral tissue following injury in models of SUI.

To fill this critical gap in knowledge, the aim of this study was to assess gene expression modulation in xenograft hMSCs, and recipient urethral tissue over the first 72 h of urethral injury. Our study of DEGs in hMSC treated, versus hMSC untreated injured urethral tissue, identified significant transcriptome profile differences between treated and untreated urethra, temporally, and in the hMSCs themselves. DEGs in hMSC treated injured urethral tissue, and in the hMSCs applied to injured urethra, are associated with several important tissue regeneration and repair pathways and mechanisms, including: (1) wound healing, (2) angiogenesis and vasoprotection, (3) neurogenesis/neuroprotection, and (4) oxidative stress suppression; Tables 2, 3.

Wound healing

Comparing between hMSC treated injured urethra and untreated injured urethra, the DEG's pattern is indicative of increased expression of genes associated with accelerated wound healing in hMSC treated urethra.

Extracellular matrix stabilization and repair. Of the top 50 DEGs observed in our study, several are involved in wound healing through ECM and connective tissue stabilization and regeneration.

Genes increasing regeneration of ECM turnover, cell migration, and protein, including elastin, collagen, and glypicans, show increased expression in hMSC treated urethra 12 h after injury. Increased Eln expression by hMSC therapy indicates improved tissue elasticity. This observation is consistent with observations of hMSC interventions in the rat dual muscle and nerve injury UI model with increased elastogenesis,[39] as well as increase in collagen and elastin post hMSC therapy of cutaneous wounds.[40] Increased expression of *Afap1*, a connective tissue growth factor, at 12 h in hMSC treated urethra indicates enhanced tissue repair following hMSC treatment. Our data show increased *Ecm1* 36 h postinjury in hMSC treated urethra. Ecm1 is involved in ECM homeostasis, blood vessel integrity, epidermal adhesion, and keratinocyte differentiation.[41,42] Interactions with perlican, EGF, as well as other growth factors mediate these functions.[43] Also at 72 h, *Flt1* increased, which is known to induce connective tissue turnover following injury and may be a mechanism to organize growing ECM rather than fibrotic scar tissue formation. We also observed increased *Chrdl2* expression at 72 h. *Chrdl2* is potentially a *BMP2* antagonist with a role in reducing fibrosis.[44]

MSC treated urethra demonstrated decreased *ALMS1* expression at 72 h postinjury. *ALMS1* is known to upregulate collagen production. Fibroblasts from *ALMS1*-deficient patients display cytoskeleton abnormalities, impaired migration, increases cell cycle length, and resistance to apoptosis.[45] Decreased *ALMS1* expression suggests reduced collagen formation and migration with increased apoptosis in urethral tissue in opposition to the DEGs seen earlier. This suggests that hMSCs provoke ECM repair during the first 36 h postinjury, however, by 72 h this protection is lost.

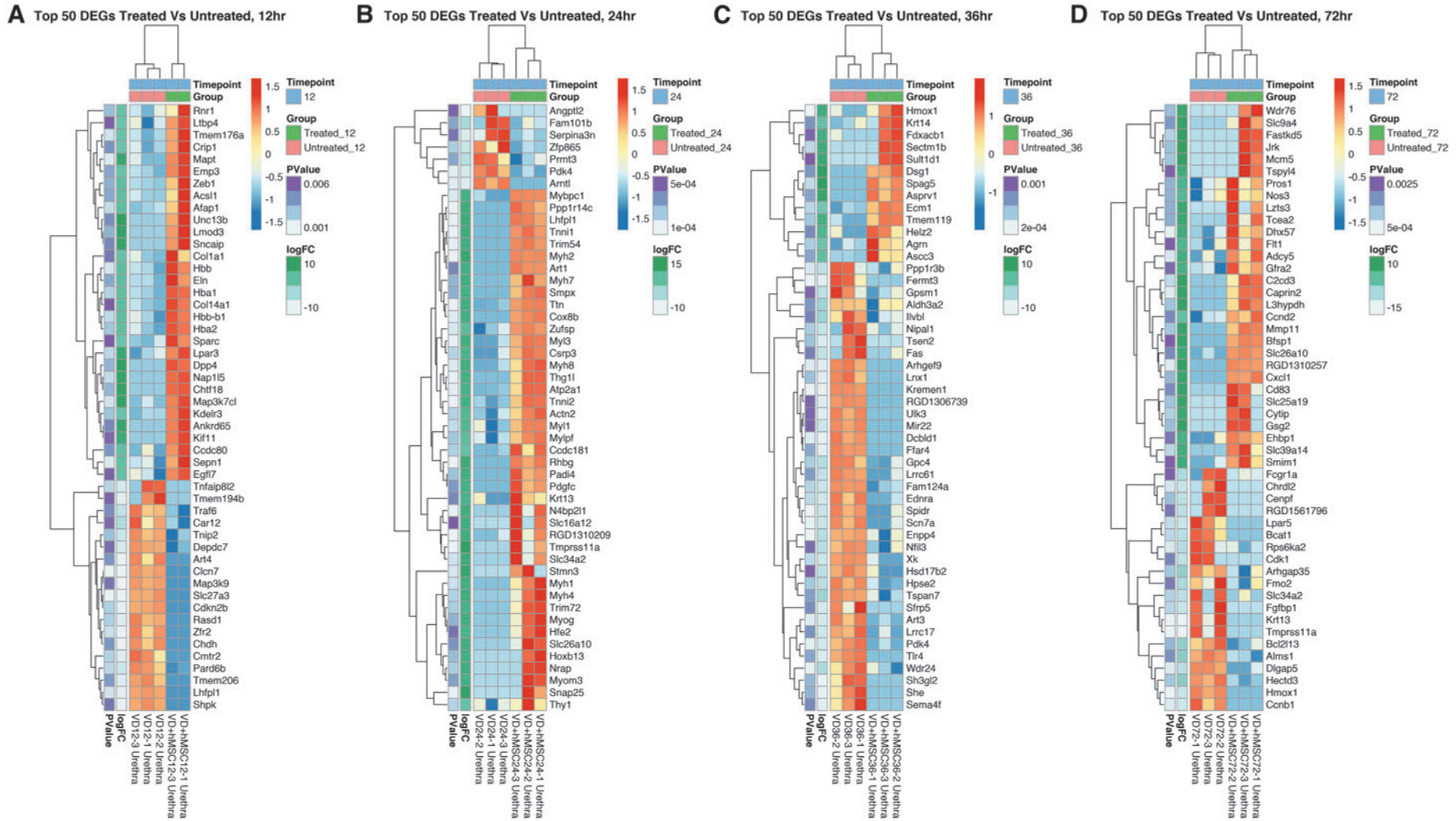

FIG. 4. Hierarchically clustered heat maps showing DEGs in hMSC treated versus untreated urethra. This figure illustrates the top 50 DEGs in hMSC treated versus untreated urethra at **(A)** 12 h, **(B)** 24 h, **(C)** 36 h, and **(D)** 72 h ranked by nominal p value (leftmost column, all $p \leq 0.05$) and FC (second column from the left). All rows are normalized (z-score) so that red coloring is upregulated versus the other group and blue is downregulated.

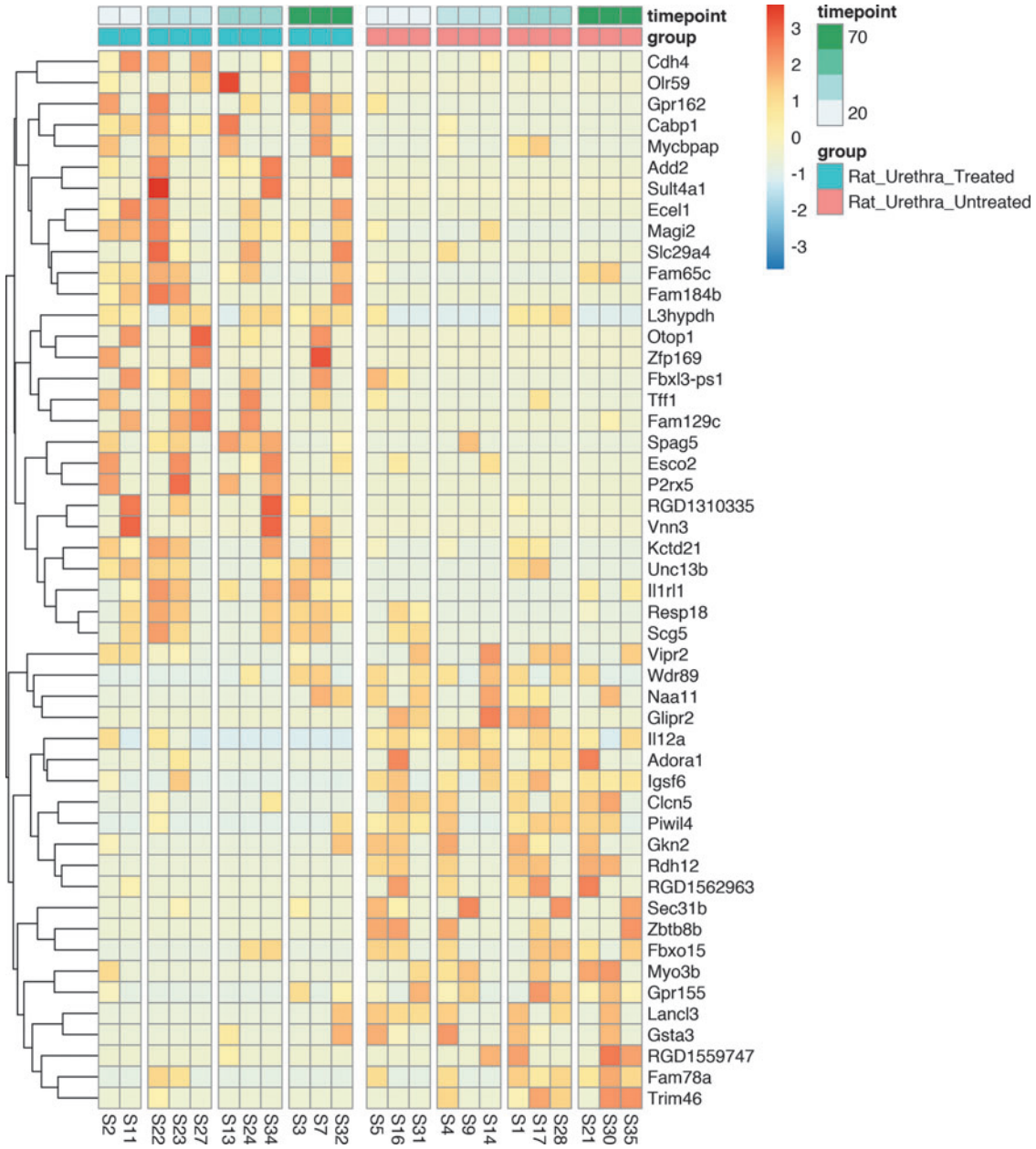

FIG. 5. Top 50 DEGs by magnitude between hMSC treated versus untreated injured urethral tissue with persistent gene expression signature across all four time points of the experiment (12, 24, 36, and 72 h post VD injury). Filtered by nominal *p* value (leftmost *column*, all $p \leq 0.05$) and ranked by FC (second *column* from the *left*). All rows are normalized (z-score) so that *red* coloring is upregulated versus the other group and *blue* is downregulated. VD, vaginal distention.

Cytokine signaling modification. *Cxcl1* and *SLC39a14* were significantly differentially expressed in hMSC treated injured urethra at all time points. Expression of *Cxcl1* increases in hMSC treated injured urethra. *Cxcl1* signal transduction occurs through *Cxcr2*.[46] *Cxcl1* is a monocyte chemoattractant and is known to enhance angiogenesis in a rat model of perfusion recovery.[47] Devalaraja *et al.*, in a study of knockout *Cxcr2* (the Cxcl1 receptor) mice demonstrated that *Cxcr2* knockout mice were wound healing impaired compared with wt mice. This was mediated through reduced neutrophil and macrophage recruitment, and impaired angiogenesis.[48] *FLT1*, also known as *VEGFR-1*, functions as a receptor for VEGF-B. FLT1 signaling upregulates urokinase-type plasminogen activator in endothelial cells consistent with a key role in ECM turnover, cell adhesion, and migration.[49]

Solute carrier (SLC) family proteins are integral membrane proteins functioning as facilitative or secondary active transporters regulating the extracellular and intracellular environment. We showed increased *SLC27a3* (at 12 h); *SLC16a12*, *SLC34a2*, and *SLC26a10* (at 24 h); and *SLC26a10*, *SLC25a19*, *SLC34a2*, and *SLC39a14* (at 72 h) expression in treated urethra. *SLC39a14* was significantly differentially expressed across all four time points. It is known that exposure of macrophages induces *SLC39a14/ZIP4* expression. *SLC39a14* knockdown results in reduced

Table 2. Laser-Captured hMSC Treated Urethra Top 50 DEGs, Which Are Known to be Involved in Wound Healing, Angiogenesis, Neurogenesis, and Antioxidative Mechanisms

Mechanism of action	*12 h post VD*	*24 h post VD*	*36 h post VD*	*72 h post VD*
Wound healing	–(+)Afap1 (connective tissue growth factor), –(+)Eln (elastin, flexible ECM molecule helping tissue returning to original shape after deformation), –(+)Ltbp4, Sparc (osteonectin, deposited by degranulating macrophages and platelets in regenerating tissue)	–(–)Arntl (or HIF1B, activates hypertrophic related genes, like MMP13, VEGFA), –(+)Csrp3 (striated muscle differentiation), –(+)Pdgfc (potent hMSC mitogen, and enhances wound repair), –(+)Thy1/CD90 (cell/cell and cell/matrix interactions, nerve regeneration, apoptosis, inflammation, fibrosis), –(+)Ttn (Titin, is a stabilizing protein in striated muscle) –(+)Myh1, Myh2, Myh4, Myh7, Myh8, Myl1, Myl3, Mylpf, and Myoh (different muscle myosin peptide genes resulting in muscle regeneration)	–(+)Ecm1 (ECM hemostasis and integrity), –(–)Gpc4 (glypicans bind growth factors and ECM molecules and participate in signal transduction cascade), –(+)Helz2 (transcriptional coactivator)	–(–)Alms1 (upregulates collagen production, less apoptosis), –(–)Bcat1 (proliferation, cell migration), –(–)Bcl2l13 (proapoptotic, induces microbial permeability), –(–)Cdk1 (cell cycle regulation), –(+)Chrdl2 (potential BMP2 antagonist – antifibrosis), –(+)Cxcl1 (neutrophil/macrophage recruitment inducing wound healing), –(+)Flt1 (VEGF-B receptor, helping ECM turnover, cell migration), –(+)Mcm5 (cell cycle progression marker G0 to G1/S phase), –(+)Slc39a14 (SLC family mediates cellular metal transporters, activates macrophage cytokine production)
Angiogenesis/ vasoprotection	–(–)Cdnk2b (anti apoptosis of vascular smooth muscle), –(+)Egfl7 (vascular remodeling, chemoattractant to endothelial cells), –(–)Traf6 (induces HIF1a expression and angiogenesis), –(+)Zeb1 (induces capillary tube formation)	–(–)Angptl2 (secreted from prevascular tissue, induces vascular proliferation, increases vascular stiffness)	–(–)Ednra (receptor of potent vasoconstrictor endothelin 1), –(+)Pros1 (protein S involved in anticoagulation, inflammation, and angiogenesis in wound healing)	–(+)Cxcl1 (enhances arteriogenesis)
Neuroprotective/ neurogeneration	–(+)Acsl1	–(+)Atp2a1 (intracellular Ca pump involved in muscular contraction)	–(+)Agrn (induces Ach receptor clustering in muscle), –(–)Hpse2 (in pelvic ganglia neural cell bodies potentially plays a necessary role in complete bladder voiding), –(–)Nfil3 (neuroprotective, specially against immune-mediated inflammation)	–(+)Cd83 (dendritic cells marker), –(+)Gfra2 (neurotrophic factor, helps resolving local neural tissue damage)
Antioxidative stress	—	–(+)Atp2a1 (reduces hydroxyl radical injury)	–(+)Hmox1 (antioxidant, increases anti-inflammatory cytokine IL-10, and IL-1Ra)	–(+)Adcy5, –(+)Nos3 (suppresses inflammation following ischemia/reperfusion injury, however, it can induce more apoptosis as well)

(+ or – demonstrates increase or decrease in gene expression).
ECM, extracellular matrix; hMSC, human mesenchymal stem cell; SLC, solute carrier; VD, vaginal distention; VEGF, vascular endothelial growth factor.

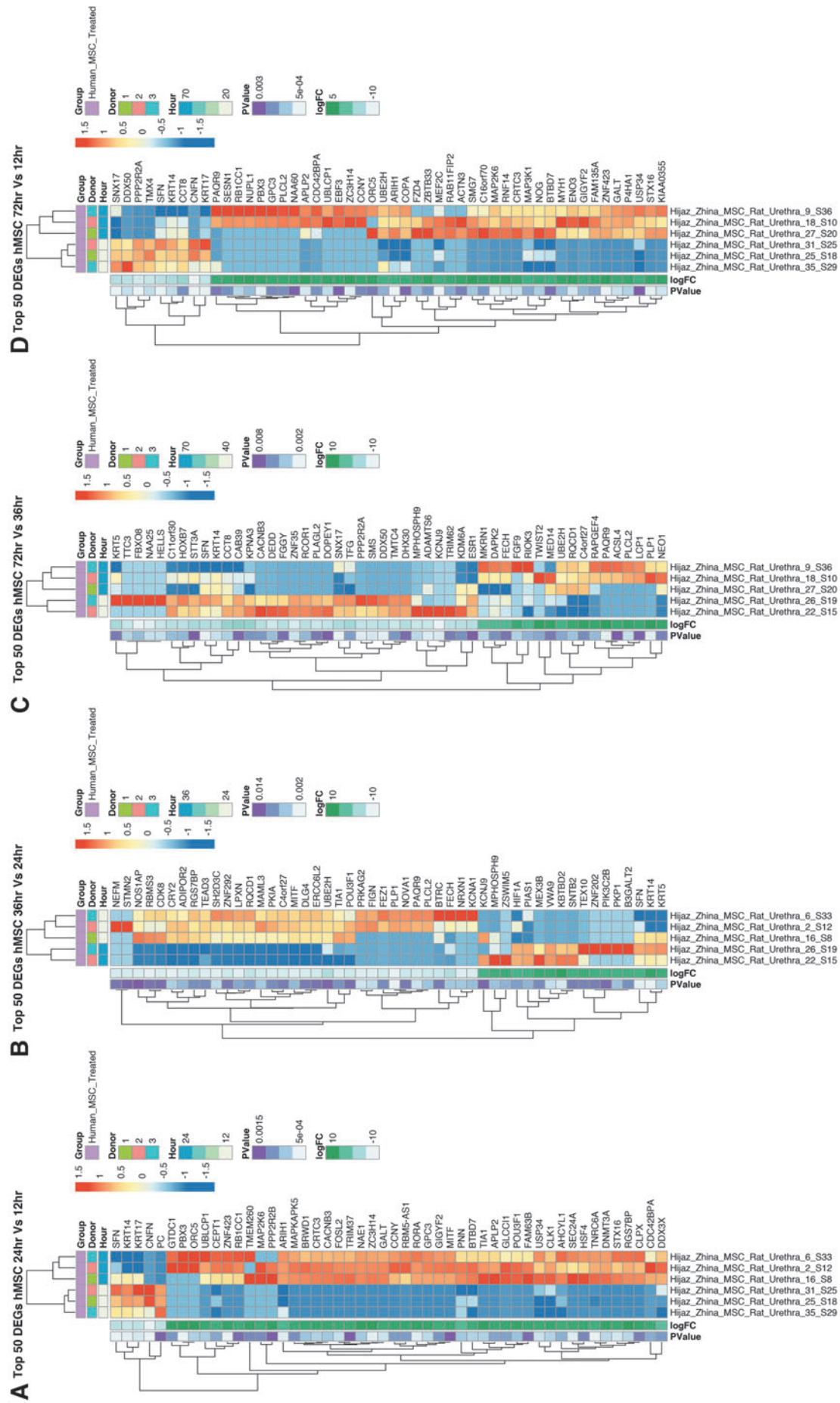

FIG. 6. The top 50 DEGs between gene expression in laser-captured hMSCs from injured urethra in pairs of consecutive time points ([**A**] 12 vs. 24 h, [**B**] 24 vs. 36 h, [**C**] 36 vs. 72 h, and [**D**] 12 vs. 72 h) postinjury. Comparison shows a persistently altered gene expression signature. Ranked by nominal p value (leftmost *column*, all $p \leq 0.05$). All rows are normalized (z-score) so that *red* coloring is upregulated versus the other group and *blue* is downregulated.

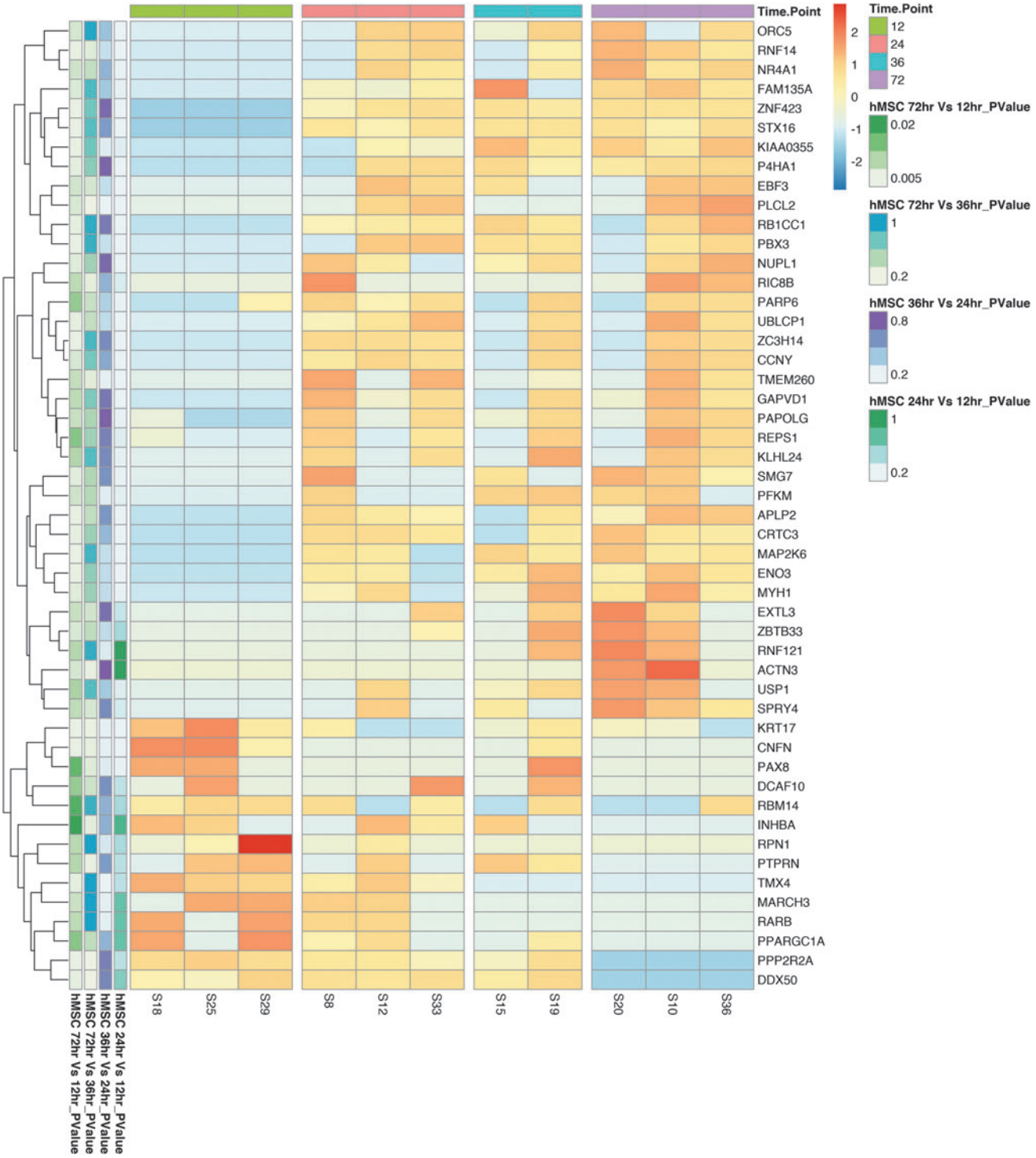

FIG. 7. Top 50 DEGs by magnitude between laser-captured hMSCs from injured urethral tissue within which expression changes greatly over the time course of 72 h filtered by nominal *p* value (leftmost *column*, all $p \leq 0.05$) and ranked by FC (second *column* from the *left*). All rows are normalized (z-score) so that *red* coloring is upregulated versus the other group and *blue* is downregulated.

macrophage cytokine expression implicating hMSCs in the activation of macrophage cytokine production.[50]

We observed increased *Afap1* and *Ltbp4* expression at 12 h in hMSC treated injured urethra. *Afap1* binds to Src and is required for Src activation by TGF-β1 and CCN2. Knockdown of *AFAP1* blocks Src promoter activity to TGF-β1 and CCN2 exposure in osteoblast cultures.[51] On the other hand, *Ltbp4* knockdown in fibroblasts caused reduced cell surface expression of TGFβ receptors.[52] Based on this evidence, increased *Afap1* and *Ltbp4* expression likely increases TGF-β signaling, consistent with hMSCs.

Table 3. Laser-Captured hMSCs from Injured Urethra Top 50 DEGs Comparing Consecutive Time Points in Acute Phase of Injury (12 Versus. 24 h, 24 Versus 36 h, 36 Versus 72 h, and 12 Versus 72 h) Demonstrates Genes, Which Are Known to be Involved in Wound Healing, Angiogenesis, Neurogenesis, and Antioxidative Mechanisms

Mechanism of action	*Comparing 12 vs. 24 h post VD*	*Comparing 24 vs. 36 h post VD*	*Comparing 36 vs. 72 h post VD*	*Comparing 12 vs. 72 h post VD*
Wound healing	–(+)DDX3X (replication-linked DNA damage repair) –(+)GPC3 (Glypican3 may interact with FZD in stem cell fate decisions during development and injury resolution) –(+) MAP2K6, and MAPKAPK5 (Directs cellular responses to stimuli, regulates proliferation, gene expression, differentiation, mitosis, cell survival, and apoptosis) –(+)ZNF423 (Interactions of SMADs 1–4 with ZNF423 are important in BMP2/4/7 signal transduction as well as interacting with the Notch intracellular domain)	–(−)FIGN (microtubule severing factor) –(−)MAML3 (mastermind-like transcriptional coactivator 3) –(+)PIK3C2B (play roles in signaling pathways involved in cell proliferation, cell survival, cell migration, intracellular protein trafficking) –(+)TEX10 (immunoprecipitates with SOX2 and is necessary for self-renewal and pluripotency of embryonic stem cells) –(+)ZNF202, ZNF292	–(+)DAPK2 (helps granulocytic chemotactic response) –(−)ESR1 (estrogen receptor 1) –(−)KDM6A (removes histone-3 trimethylation allowing transcriptional activation, activates regeneration) –(+)NEO1 (involved in cell proliferation, differentiation, and migration) –(−)ZNF35	–(+)FZD4 (helps injury response through WNC/B-catenin pathway) –(+)MAP2K6, and (+)MAP3K1 (directs cellular responses to stimuli regulates proliferation, gene expression, differentiation, mitosis, cell survival, and apoptosis –(+)MYH1 (myosin heavy chain 1) –(+)NOG (niggin is a BMP antagonist, and it is involved in the development of many body tissues, including nerve tissue, muscles, and bones) –(+)P4HA1 (hypoxia upregulates P4HA1, which in turn plays a role in type 2 collagen synthesis and ECM remodeling) –(+)ZNF423 (Interactions of SMADs 1–4 with ZNF423 are important in BMP2/4/7 signal transduction as well as interacting with the Notch intracellular domain)
Angiogenesis/ Vasoprotection	—	–(+)HIF1A (expression in response to hypoxic stress leads to upregulation of VEGFA)	–(+)FGF9 (enhances microvessel formation, vasoreactivity, smooth muscle covering) –(−)HOXB7 (Homebox B7, promotes angiogenesis through upregulation of FGF, CXCL1, VEGFA, and IL-8)	–(+)MEF2C (negative regulator of angiogenic budding, gets suppressed in hypoxic condition) –(+)P4HA1 (hypoxia upregulates P4HA1, which in turn plays a role in neovascularization)-(+)RAB11FIP2 (loss of RAB11FIP2 is associated with increased vascular endothelial permeability)

(*continued*)

TABLE 3. (CONTINUED)

Mechanism of action	*Comparing 12 vs. 24 h post VD*	*Comparing 24 vs. 36 h post VD*	*Comparing 36 vs. 72 h post VD*	*Comparing 12 vs. 72 h post VD*
Neuroprotective/ Neurogeneration	—	–(+)HIF1A (expression in response to hypoxic stress leads to stimulated motor neuron regeneration, accelerated neuromuscular junction reinnervation) –(–)KCNA1, (+) KCNJ9 (K voltage-gated channel contributes to the regulation of the membrane potential and nerve signaling, and prevents neuronal hyperexcitability) –(–)NEFM (neurofilament medium a biomarker of neural damage) –(–)STMN2 (adipose-derived hMSC upregulates STMN2. It is upregulated in regenerating sensory axons following nerve crush injury) –(–)PAQR9 (Progestin and AdipoQ Receptor Family Member 9)	–(–)KCNJ9 (K voltage-gated channel contributes to the regulation of the membrane potential and nerve signaling, and prevents neuronal hyperexcitability) –(+)PAQR9 (Progestin and AdipoQ Receptor Family Member 9)	–(+)PAQR9 (Progestin and AdipoQ Receptor Family Member 9)

(+ or – demonstrates increase or decrease in gene expression).
ZNF, zinc finger.

MSC treated injured urethra expresses reduced *GPC4* at 36 h. *GPC4* is a glypican. These molecules bind growth factors and ECM molecules and participate in signal transduction cascades.[53] Decreased *Gpc4* expression in hMSC treated injured urethra results in decreased signal transduction in injured urethral tissue. The signaling cascade response postinjury might overwhelm injured tissue cells. We speculate this unexpected result implicates that hMSC treatment focuses host tissue cells on injury resolution rather than enhancing an inflammatory signaling cascade released immediately following injury.

Cell cycle regulation. Of the top DEGs, we observed several cell cycle regulatory genes. *Pdgfc* expression increased at 24 h in hMSC treated urethra and is a mesenchymal cell mitogen. In a diabetic mouse model of delayed wound healing, exogenous PDGF-CC significantly enhanced repair of full-thickness skin excisions.[54] Similarly, Helz2 is a transcriptional coactivator and increases expression in hMSC treated injured urethra at 36 h. During 3T3-L1 preadipocyte differentiation, HELZ2 and THRAP3 interactions lead to enhanced PPARγ-mediated gene activation.[55] Mcm5 is a cell cycle progression marker (G0 to G1/S phase transition) of cardiomyocytes in a zebrafish model of cryoinjury.[56] Increased expression of *Mcm5* expression is also observed at 72 h in treated urethral tissue suggesting enhanced cell proliferation in hMSC treated host urethra. Unexpectedly, decreased expression of several genes associated with proliferation and cell cycle control was observed in treated urethral tissue; *Arntl* (at 24 h); and Bcat1 and Cdk1 (at 72 h). *Arntl* shows decreased expression at 24 h in hMSC treated urethra postinjury. Arntl, also known as Hif-1β, activates hypertrophic related genes like *MMP13*, *COL10A1*, and *VEGFA* when dimerized with Hif-2α; however, competitive binding by Hif-3α suppresses transcriptional activation.[57] Knockdown of *BCAT1* expression reduced proliferation, cell migration, and invasion of human nasopharyngeal carcinoma cells.[58] CDK1 is involved in cell cycle regulation, specifically the G1 to S transition. Decreased expression of these genes was seen in treated urethra. This is counterintuitive considering evidence of increased expression of *Pdgfc*, *Helz*, and *Mcm5*. Ultimately, this may be evidence that cell cycle regulation and proliferation during wound resolution is cell type specific and modulated by hMSC treatment. As the time point of significant increase in cell cycle progression genes was observed, generally after 24 h, this could show hMSC treated host tissue initially concentrates on survival before switching to proliferation late.

Looking at the top differentially expressed hMSC genes (at consecutive time points) obtained from hMSCs within injured urethra (Table 3), we see increased expression of cell cycle and transcriptional regulation, cell migration, and signal transduction genes. In harvested hMSCs, a variety of zinc finger (ZNF) proteins exhibit increased expression throughout the study, such as increased expression of *ZNF423* (24 h); *ZNF202* and *ZNF292* (36 h); and *ZNF423* and *ZSWIM5* (72 h) in treated urethra. ZNF transcription factors are involved in the regulation of several cellular processes. ZNFs are implicated in transcriptional regulation, ubiquitin-mediated protein degradation, signal transduction, actin targeting, DNA repair, cell migration, and numerous other processes.[59] SMADs 1–4 interactions with ZNF423 are important in BMP2/4/7 signal transduction as well as interacting with the Notch intracellular domain.[60] Knockdown of *ZNF423* expression in neuroblastoma cells leads to a proliferative advantage and decreased differentiation in response to retinoic acid while overexpression resulted in reduced proliferation and increased retinoic acid-mediated differentiation.[61]

The wnt/β-catenin pathway is also important to injury response.[62] Disruption of wnt/β-catenin signaling through *Fzd4* mutation led to the persistence of epithelial injury in mice lacking Fzd4 following ischemia reperfusion injury.[63] *FZD4* is differentially expressed in hMSCs between 72 and 36 h. On the other hand, increased *GPC3* expression in hMSCs between 24 to 12 h may interact with FZD receptor in stem cell fate decisions during development and injury resolution.[64] As mentioned above, glypicans play a critical role in cell growth during development.

Muscle differentiation and stabilization. Genes involved in muscle differentiation and stabilization were observed in the top DEGs. Increased gene expression of these genes was observed in treated urethral tissue. Csrp3 is involved in regulation of myogenic differentiation in striated muscles as observed in a Drosophila homolog knockout model.[65] TTN is a stabilizing protein of striated muscle.[66] Our results identify several differentially expressed myosin peptides in treated urethral tissue at 24 h postinjury. They include *MYH1*, *MYH2*, *MYH4*, *MYH7*, *MYH8*, *MYL1*, *MYL3*, *MYLPF*, and *MYOG*. Increased expression of myosin peptides indicate enhanced muscular regeneration occurring in treated urethral tissue.

Angiogenesis and vasoprotection

Stimulation of angiogenesis and suppression of fibrosis in injured tissue has been reported in several animal models of hMSC therapy, including cardiac repair after experimental myocardial infarction,[67] cutaneous wound healing through increase of VEGF and HGF,[68] IGF-1m PDGF-B, and Ang-1,[69] and lung fibrosis/injury models.[70] Our result demonstrates that hMSC treated urethra increased expression of several proangiogenic factors, including *Egfl7* and *Zev1* (at 12 h); *Pros1* (at 36 h); and *Cxcl1* (at 72 h). While other genes known to be involved in angiogenesis are downregulated, including *Cdkn2b* and *Traf6* (at 12 h); *Angptl2* (at 24 h); and *Ednra* (at 36 h) (Table 2).

On the other hand, hMSCs captured from injured urethra show significant decrease of *HOXB7* expression at 72 h compared with 36 h postinjury. *HBOX7* promotes a switch to active angiogenesis through FGF, VEGFA, IL-8, and CXCL1[71] as reviewed in Kachgal *et al*.[72] Timing of decrease in expression of *HOXB1* (72 h compared with 36 h) and increase in expression of *CXCL1* (at 72 h) suggests that HOXB1 may primarily increase *CXCL1* expression by 72 h postinjury, but this increase in *CXCL1* expression would also act as a negative autoregulatory feedback to decrease *HOXB1* expression at 72 h and hence may result in controlled angiogenesis.

Endothelial cells express *EGFL7* during vascular remodeling and acts as a chemoattractant to endothelial cells.[73] Endothelial cells upregulate expression of *EGFL7* following arterial injury.[73] Conditioned media from the metastatic

breast cancer cell line, MDA-MB-231, induced capillary tube formation in HUVECs; however both *ZEB1* knockdown and VEGFA neutralizing antibody suppressed tube formation.[74] PROS1 participates in anticoagulation, inflammation, and angiogenesis during wound resolution as reviewed in Suleiman *et al*.[75] Increase in expression of *EGFL7* (at 12 h) and *PROS1* (at 36 h) treated urethra could promote increased angiogenesis in urethral tissue.

Our finding of decreased *Angptl2* expression is inconsistent with the results of Chen *et al.*,[69] in which increased *ANG-1* was observed following hMSC therapy of cutaneous wounds resulting in enhanced proliferation of endothelial cells and neovascularization. Moreover, *Angptl2* has been suggested to have a role in inducing proliferation and migration of vascular smooth muscle cells of the vascular intima,[76] also in inducing inflammatory fibrosis,[77] and serum ANGPTL2 levels positively correlate with aortic stiffness and mortality in human kidney transplant patients.[78] Our finding of decrease in *Angptl2* expression in hMSC treated urethra suggests hMSC treatment might be evidence for decreased urethral tissue fibrosis and increased vascular wall flexibility during healing.

In a vascular injury model of mice in which aortic aneurysms were generated with porcine pancreatic elastase, *Cdkn2b* knockout mice developed larger aortic aneurysms yet smooth muscle proliferation was unexpectedly normal. The authors determined this was due to increased apoptosis in smooth muscle cells.[79] We observed decreased *Cdkn2b* expression in treated urethral tissue. This could result in decreased stiffness of vascular wall with decreased smooth muscle cell proliferation in the neovasculature of recovering urethra.

Reduced *Ednra* expression is seen at 36 h postinjury in treated urethra. Endothelin 1, a ligand of EDNRA, is a potent vasoconstrictor and is used in animal models to stimulate ischemic strokes in brain and induce peripheral neuropathy of the sciatic nerve.[80,81] Decreased *Ednra* expression may diminish the vasoconstriction in injured urethra, which might result in enhanced blood flow within the injured tissue.

HIF1a, depletion in myeloid cells, accelerates renal fibrosis in a mouse model of obstructive nephropathy.[82] Peripheral neuronal expression of *HIF1a*, in response to hypoxic stress, leads to upregulation of VEGFA, stimulated motor neuron regeneration, and accelerated neuromuscular junction reinnervation.[83] We found increased *HIF1a* expression in captured hMSC at 36 h compared with 24 h postinjury.

Our result shows hMSC increased *FGF9* expression at 72 h compared with 36 h. Microvessel formation in the presence of FGF9-seeded hydrogels enhances flow, vasoreactivity, and smooth muscle covering.[84] *P4HA1* expression increases in hMSCs captured from injured urethra at 72 h compared with 12 h. This finding is consistent with previous studies showing hypoxia upregulates *P4HA1*, which in turn enhances neovascularization, type 2 collagen synthesis, and ECM remodeling.[85–87]

Neurogenesis and neuroprotection

Our data show evidence of DEGs from treated urethra compared with untreated urethra involved in neurogenesis and neuroprotection. These genes include *Acsl1*, *Atp2a1*, *Agrn*, *Hpse2*, *Nfil3*, *Cd83*, and *Gfra2* and were increased in treated urethral tissue. Overexpression of *Acsl1* is protective of Schwann cells from oxidative stress and mitochondrial dysfunction.[88] *Atp2a1* is an intracellular Ca^{+} pump involved in muscular excitation and contraction.[89] Also, *Atp2a1* overexpression reduced hydroxyl radical injury in murine myocardium directly exposed to hydroxyl radicals.[90] *Agrn* is a component of the synaptic basal lamina and induces acetylcholine receptor clustering in muscle fiber.[91] Loss of function mutations in *Hpse2* leads to urofacial syndrome and are characterized by grimacing and incomplete bladder emptying. *Hpse2* is observed in pelvic ganglia neural cell bodies and potentially plays a necessary role in complete bladder voiding.[92] Neuronal expression of *Nfil3* in a mouse model of ALS reduced excitotoxic neuronal damage and protects neurons against neurodegeneration; this suggests a protective role for *Nfil3* against immune-mediated inflammation.[93] CD83 is a cell surface marker of dendritic cells,[94] and increased *CD83* expression in hMSC treated injured urethra suggests increased neuroregeneration. Following a surgical model of spinal cord injury, *GFRA2* expression is reduced suggesting a failure of these cells to recruit local stem cells capable of resolving neural tissue damage.[95] Thus, increased *GFRA2* expression in treated urethral tissue is evidence of enhanced neurogenesis.

Similarly, laser-captured hMSCs showed increased expression of genes known to enhance neurogenesis and neuroprotection, including *HIF1A*, *KCNA1*, *KCNJ9*, *NEFM*, *STMN2*, *PAQR9*, and *ACSL4* when gene expression is compared over consecutive time points. *HIF1A* depletion in macrophages accelerates renal fibrosis in a mouse model of obstructive nephropathy.[82] Peripheral neuronal expression of *HIF1A*, in response to hypoxic stress, leads to upregulation of *VEGFA*, stimulated motor neuron regeneration, and accelerates neuromuscular junction reinnervation.[83] *KCNA1* and *KCNJ9* are potassium voltage-gated channel subfamily A members. The voltage-gated potassium channel mediates transmembrane potassium transport in excitable membranes, primarily in the brain and the central nervous system, but also in the kidney.[96] Voltage-gated potassium channels contribute regulation of membrane potential, nerve signaling, and prevent neuronal hyperexcitability.[97] *KCNJ9* was significantly differentially expressed comparing between 24 versus 36 h, and 36 versus 72 h. *PAQR9* is a mediator of nonclassical antiapoptotic actions of neurosteroids in the central nervous system.[98] Increased *PAQR9* expression is persistently observed in captured hMSCs from treated urethral tissue (differentially expressed comparing 12 vs. 24 h, 24 vs. 36 h, and 36 vs. 72 h) suggesting neuroprotection by hMSC treatment.

Oxidative stress modification

MSC treated injured urethral tissue also show increased expression of some genes involved in decreased oxidative stress, and inflammatory factors. In our top 50 DEGs, these include *Atp2a1*, *Hmox1*, *Adcy5*, and *Nos3*. *ATP2A1* is an intracellular Ca^{+} pump involved in muscular excitation and contraction.[89] Also, *Atp2a1* overexpression reduced hydroxyl radical injury in murine myocardium directly exposed to hydroxyl radicals.[90] Enhanced *Hmox1* expression

attenuates oxidant injury in human hepatocytes.[99] Inhibition of *Adcy5* enhances longevity and prevents oxidative stress in KO mice; overexpression led to exacerbated age-related cardiomyopathy.[100] In an inducible *Nos3* deficiency model of mouse hepatic ischemia/reperfusion injury, depletion of *Nos3* suppressed *MMP-9* expression in macrophages and neutrophils suggesting a role in suppressing inflammation following ischemia/reperfusion injury.[101] The response to doxorubicin-induced cardiac injury in *NOS3*-deficient mice was compared with that of mice with cardiomyocyte-specific overexpression of *NOS3*; *NOS3* overexpressing mice showed more cell death and reduced cardiac function than *NOS3*-deficient mice.[102]

Our study was limited by a small sample size and an animal model with uncertain generalizability to birth trauma in humans. Also, we have mainly focused on the top 50 DEGs in each time point or group comparison in overview of the larger dataset. Our results, however, are the first comprehensive transcriptomic analysis of hMSC treatment of postpartum SUI to our knowledge. Our data, therefore, represent an important resource for the field in highlighting the many signaling molecules that dynamically change expression during acute injury both with the injury alone as well as following hMSC treatment. We contend that these gene expression differences represent candidate host tissue biomarkers implicated in the control of injured tissue repair, particularly in the regulation of coagulation, stabilization of ECM pH and solute concentration, blood flow, and neuronal signaling, suppression of oxidative stress, and regulating apoptosis. Our gene expression profile data also suggest in the first 72 h postinjury, the pace and direction of healing processes are altered significantly across different time points.

Conclusions

In conclusion, our study supports the overwhelming historical evidence showing hMSC treatment alters tissue response to acute injury and improves long-term tissue function. Comparing DEGs in hMSCs between consecutive time points (12 vs. 24 h, 24 vs. 36 h, 36 vs. 72 h, and 12 vs. 72 h) we identified candidate genes involved in tissue injury that clustered by injury and hMSC treatment. This highlights the dynamic gene expression changes in hMSCs related to DNA damage repair, stem cell fate/regulation, cell survival/apoptosis, self-renewal, cell proliferation, transcription activation, migration, and injury response. Our study shows how exposure to the injured urethral environment altered gene expression within hMSCs. While further research is needed to confirm the target genes we have identified, our study represents important transcriptomic evidence for hMSC/injured tissue crosstalk and is a novel resource that identifies new therapeutic targets for postpartum SUI therapy and prevention.

Acknowledgments

The authors thank the CWRU Genomics Core and Applied Functional Genomics Core for helping with the RNA-Seq. The authors specially thank Ilaha Isali, MD for assisting with the animal phase of the study.

Author Contributions

Z.S.: Conception and design, provision of study material, collection and assembly of data, data analysis and interpretation, and article writing; J.K.: Conception and design, data interpretation, and article writing; B.R.: Collection and assembly of data, data analysis and interpretation, and article writing; A.K.: Provision of study material, and collection of data; M.C.: Collection and assembly of data; M.J.C.: Collection and assembly of data, data analysis and interpretation, and article writing; A.C.: Conception and design, and final approval of article; B.C.: Article writing and review; A.H.: Conception and design, financial support, and final approval of article.

Disclosure Statement

No competing financial interests exist with the CWRU authors.

Funding Information

Financial support for this project was provided by the Virginia and David Baldwin fund, a grant from NIH/NIBIB P41EB021911, and by the University Hospitals of Cleveland Urology Institute.

Supplementary Material

Supplementary Table S1
Supplementary Table S2

References

1. Minassian, V.A., Drutz, H.P., and Al-Badr, A. Urinary incontinence as a worldwide problem. Int Jof Gynecol Obstet **82,** 327, 2003.
2. Brubaker, L. Postpartum urinary incontinence. BMJ **324,** 1227, 2002.
3. Delancey, J.O., Kane Low, L., Miller, J.M., Patel, D.A., and Tumbarello, J.A. Graphic integration of causal factors of pelvic floor disorders: an integrated life span model. Am J Obstet Gynecol **199,** 610.e1, 2008.
4. Dietz, H.P. Pelvic floor trauma in childbirth. Aust N Z J Obstet Gynaecol **53,** 220, 2013.
5. Dietz, H.P., and Wilson, P.D. Childbirth and pelvic floor trauma. Best Pract Res Clin Obstet Gynaecol **19,** 913, 2005.
6. de Araujo, C.C., Coelho, S.A., Stahlschmidt, P., and Juliato, C.R.T. Does vaginal delivery cause more damage to the pelvic floor than cesarean section as determined by 3D ultrasound evaluation? A systematic review. Int Urogynecol J **29,** 639, 2018.
7. Baessler, K., and Schuessler, B. Childbirth-induced trauma to the urethral continence mechanism: review and recommendations. Urology **62,** 39, 2003.
8. Zambon, J.P., Matthews, C.A., and Badlani, G.H. Midurethral slings. J Endourol **32,** S105, 2018.
9. U.S. Food and Drug Administration. Urogynecologic surgical Mesh implant. 2019. Available at https://www.fda.gov/medical-devices/implants-and-prosthetics/urogynecologic-surgical-mesh-implants (accessed June 22, 2020).
10. Caplan, A.I. What's in a name? Tissue Eng Part A **16,** 2415, 2010.

11. Tran, C., and Damaser, M.S. The potential role of stem cells in the treatment of urinary incontinence. Ther Adv Urol **7,** 22, 2015.
12. Gotoh, M., Yamamoto, T., Kato, M., *et al*. Regenerative treatment of male stress urinary incontinence by periurethral injection of autologous adipose-derived regenerative cells: 1-year outcomes in 11 patients. Int J Urol **21,** 294, 2014.
13. Sadeghi, Z., Isariyawongse, J., Kavran, M., *et al*. Mesenchymal stem cell therapy in a rat model of birth-trauma injury: functional improvements and biodistribution. Int Urogynecol J **27,** 291, 2016.
14. Ayala-Cuellar, A.P., Kang, J.H., Jeung, E.B., and Choi, K.C. Roles of mesenchymal stem cells in tissue regeneration and immunomodulation. Biomol Ther (Seoul) **27,** 25, 2019.
15. Wakabayashi, K., Nagai, A., Sheikh, A.M., *et al*. Transplantation of human mesenchymal stem cells promotes functional improvement and increased expression of neurotrophic factors in a rat focal cerebral ischemia model. J Neurosci Res **88,** 1017, 2010.
16. Togel, F., Weiss, K., Yang, Y., Hu, Z., Zhang, P., and Westenfelder, C. Vasculotropic, paracrine actions of infused mesenchymal stem cells are important to the recovery from acute kidney injury. Am J Physiol Renal Physiol **292,** F1626, 2007.
17. Rehman, J., Traktuev, D., Li, J., *et al*. Secretion of angiogenic and antiapoptotic factors by human adipose stromal cells. Circulation **109,** 1292, 2004.
18. Togel, F., Hu, Z., Weiss, K., Isaac, J., Lange, C., and Westenfelder, C. Administered mesenchymal stem cells protect against ischemic acute renal failure through differentiation-independent mechanisms. Am J Physiol Renal Physiol **289,** F31, 2005.
19. Lange, C., Togel, F., Ittrich, H., *et al*. Administered mesenchymal stem cells enhance recovery from ischemia/reperfusion-induced acute renal failure in rats. Kidney Int **68,** 1613, 2005.
20. Fuse, K., Kodama, M., Hanawa, H., *et al*. Enhanced expression and production of monocyte chemoattractant protein-1 in myocarditis. Clin Exp Immunol **124,** 346, 2001.
21. Xu, X., Xu, Z., Xu, Y., and Cui, G. Effects of mesenchymal stem cell transplantation on extracellular matrix after myocardial infarction in rats. Coron Artery Dis **16,** 245, 2005.
22. Bai, L., Lennon, D.P., Caplan, A.I., *et al*. Hepatocyte growth factor mediates mesenchymal stem cell-induced recovery in multiple sclerosis models. Nat Neurosci **15,** 862, 2012.
23. Constantin, G., Marconi, S., Rossi, B., *et al*. Adipose-derived mesenchymal stem cells ameliorate chronic experimental autoimmune encephalomyelitis. Stem Cells **27,** 2624, 2009.
24. Lennon, D.P., and Caplan, A.I. Isolation of human marrow-derived mesenchymal stem cells. Exp Hematol **34,** 1604, 2006.
25. Horan, P.K., and Slezak, S.E. Stable cell membrane labelling. Nature **340,** 167, 1989.
26. Jiang, H., Lei, R., Ding, S.-W., and Zhu, S. Skewer: a fast and accurate adapter trimmer for next-generation sequencing paired-end reads. BMC Bioinformatics **15,** 182, 2014.
27. Kim, D., Langmead, B., and Salzberg, S.L. HISAT: a fast spliced aligner with low memory requirements. Nature Methods **12,** 357, 2015.
28. Li, H., Handsaker, B., Wysoker, A., *et al*. The sequence alignment/map format and SAMtools. Bioinformatics **25,** 2078, 2009.
29. Liao, Y., Smyth, G.K., and Shi, W. featureCounts: an efficient general purpose program for assigning sequence reads to genomic features. Bioinformatics **30,** 923, 2014.
30. Robinson, M.D., McCarthy, D.J., and Smyth, G.K. edgeR: a Bioconductor package for differential expression analysis of digital gene expression data. Bioinformatics **26,** 139, 2010.
31. Hänzelmann, S., Castelo, R., and Guinney, J. GSVA: gene set variation analysis for microarray and RNA-Seq data. BMC Bioinformatics **14,** 7, 2013.
32. de Oliveira, S., Rosowski, E.E., and Huttenlocher, A. Neutrophil migration in infection and wound repair: going forward in reverse. Nat Rev Immunol **16,** 378, 2016.
33. Aydemir, T.B., and Cousins, R.J. The multiple faces of the metal transporter ZIP14 (SLC39A14). J Nutr **148,** 174, 2018.
34. Caplan, A.I. Mesenchymal stem cells. J Orthop Res **9,** 641, 1991.
35. Gnecchi, M., Zhang, Z., Ni, A., and Dzau, V.J. Paracrine mechanisms in adult stem cell signaling and therapy. Circ Res **103,** 1204, 2008.
36. Caplan, A.I. MSCs as therapeutics. In: Hematti, P., Keating, A., eds. Mesenchymal Stromal Cells: Biology and Clinical Applications. New York, NY: Springer New York, 2013. p. 79.
37. Caplan, A.I., and Hariri, R. Body management: mesenchymal stem cells control the internal regenerator. Stem Cells Transl Med **4,** 695, 2015.
38. Caplan, A.I. New MSC: MSCs as pericytes are Sentinels and gatekeepers. J Orthop Res **35,** 1151, 2017.
39. Deng, K., Lin, D.L., Hanzlicek, B., *et al*. Mesenchymal stem cells and their secretome partially restore nerve and urethral function in a dual muscle and nerve injury stress urinary incontinence model. Am J Physiol Renal Physiol **308,** F92, 2015.
40. Kwon, D.S., Gao, X., Liu, Y.B., *et al*. Treatment with bone marrow-derived stromal cells accelerates wound healing in diabetic rats. Int Wound J **5,** 453, 2008.
41. Han, Z., Ni, J., Smits, P., *et al*. Extracellular matrix protein 1 (ECM1) has angiogenic properties and is expressed by breast tumor cells. FASEB J **15,** 988, 2001.
42. Sercu, S., Zhang, M., Oyama, N., *et al*. Interaction of extracellular matrix protein 1 with extracellular matrix components: ECM1 is a basement membrane protein of the skin. J Invest Dermatol **128,** 1397, 2008.
43. Chan, I. The role of extracellular matrix protein 1 in human skin. Clin Exp Dermatol **29,** 52, 2004.
44. Nakayama, N., Han, C.-y.E., Cam, L., *et al*. A novel chordin-like BMP inhibitor, CHL2, expressed preferentially in chondrocytes of developing cartilage and osteoarthritic joint cartilage. Development **131,** 229, 2004.
45. Zulato, E., Favaretto, F., Veronese, C., *et al*. ALMS1-deficient fibroblasts over-express extra-cellular matrix components, display cell cycle delay and are resistant to apoptosis. PLoS One **6,** e19081, 2011.
46. Tsai, H.-H., Frost, E., To, V., *et al*. The chemokine receptor CXCR2 controls positioning of oligodendrocyte precursors in developing spinal cord by arresting their migration. Cell **110,** 373, 2002.
47. Vries, M.H.M., Wagenaar, A., Verbruggen, S.E.L., Molin, D.G.M., and Post, M.J. CXCL1 promotes arteriogenesis

through enhanced monocyte recruitment into the peri-collateral space. Angiogenesis **18,** 163, 2015.
48. Devalaraja, R.M., Nanney, L.B., Du, J., *et al*. Delayed wound healing in CXCR2 knockout mice. J Invest Dermatol **115,** 234, 2000.
49. Olofsson, B., Korpelainen, E., Pepper, M.S., *et al*. Vascular endothelial growth factor B (VEGF-B) binds to VEGF receptor-1 and regulates plasminogen activator activity in endothelial cells. Proc Natl Acad Sci U S A **95,** 11709, 1998.
50. Sayadi, A., Nguyen, A.T., Bard, F.A., and Bard-Chapeau, E.A. Zip14 expression induced by lipopolysaccharides in macrophages attenuates inflammatory response. Inflamm Res **62,** 133, 2013.
51. Cho, Y., Silverstein, R., Geisinger, M.T., *et al*. AFAP1 is a novel downstream mediator of TGF-β1 for CCN2 induction in osteoblasts. PLoS One **10,** e0136712, 2015.
52. Su, C.-T., Huang, J.-W., Chiang, C.-K., *et al*. Latent transforming growth factor binding protein 4 regulates transforming growth factor beta receptor stability. Hum Mol Genet **24,** 4024, 2015.
53. De Cat, B., and David, G. Developmental roles of the glypicans. Semin Cell Dev Biol **12,** 117, 2001.
54. Gilbertson, D.G., Duff, M.E., West, J.W., *et al*. Platelet-derived growth factor C (PDGF-C), a novel growth factor that binds to PDGF α and β receptor. J Biol Chem **276,** 27406, 2001.
55. Katano-Toki, A., Satoh, T., Tomaru, T., *et al*. THRAP3 interacts with HELZ2 and plays a novel role in adipocyte differentiation. Mol Endocrinol **27,** 769, 2013.
56. Chablais, F., Veit, J., Rainer, G., and Jaźwińska, A. The zebrafish heart regenerates after cryoinjury-induced myocardial infarction. BMC Dev Biol **11,** 21, 2011.
57. Markway, B.D., Cho, H., Anderson, D.E., *et al*. Hypoxia-inducible factor 3-alpha expression (HIF-3α) is associated with the stable chondrocyte phenotype and inhibits HIF-2α/ARNTL-mediated transactivation of matrix metalloproteinase-13. Osteoarthritis Cartilage **23,** A153, 2015.
58. Zhou, W., Feng, X., Ren, C., *et al*. Over-expression of BCAT1, a c-Myc target gene, induces cell proliferation, migration and invasion in nasopharyngeal carcinoma. Mol Cancer **12,** 53, 2013.
59. Cassandri, M., Smirnov, A., Novelli, F., *et al*. Zinc-finger proteins in health and disease. Cell Death Discov **3,** 17071, 2017.
60. Masserdotti, G., Badaloni, A., Green, Y.S., *et al*. ZFP423 coordinates Notch and bone morphogenetic protein signaling, selectively up-regulating Hes5 gene expression. J Biol Chem **285,** 30814, 2010.
61. Huang, S., Laoukili, J., Epping, M.T., *et al*. ZNF423 is critically required for retinoic acid-induced differentiation and is a marker of neuroblastoma outcome. Cancer Cell **15,** 328, 2009.
62. Bastakoty, D., and Young, P.P. Wnt/beta-catenin pathway in tissue injury: roles in pathology and therapeutic opportunities for regeneration. FASEB J **30,** 3271, 2016.
63. Lin, S.-L., Li, B., Rao, S., *et al*. Macrophage Wnt7b is critical for kidney repair and regeneration. Proc Natl Acad Sci U S A **107,** 4194, 2010.
64. Capurro, M., Martin, T., Shi, W., and Filmus, J. Glypican-3 binds to Frizzled and plays a direct role in the stimulation of canonical Wnt signaling. J Cell Sci **127,** 1565, 2014.
65. Arber, S., Halder, G., and Caroni, P. Muscle LIM protein, a novel essential regulator of myogenesis, promotes myogenic differentiation. Cell **79,** 221, 1994.
66. Granzier, H., and Labeit, S. Structure-function relations of the giant elastic protein titin in striated and smooth muscle cells. Muscle Nerve **36,** 740, 2007.
67. Wang, J., Najjar, A., Zhang, S., *et al*. Molecular imaging of mesenchymal stem cell: mechanistic insight into cardiac repair after experimental myocardial infarction. Circ Cardiovasc Imaging **5,** 94, 2012.
68. Lee, D.E., Ayoub, N., and Agrawal, D.K. Mesenchymal stem cells and cutaneous wound healing: novel methods to increase cell delivery and therapeutic efficacy. Stem Cell Res Ther **7,** 37, 2016.
69. Chen, L., Tredget, E.E., Wu, P.Y., and Wu, Y. Paracrine factors of mesenchymal stem cells recruit macrophages and endothelial lineage cells and enhance wound healing. PLoS One **3,** e1886, 2008.
70. Moodley, Y., Atienza, D., Manuelpillai, U., *et al*. Human umbilical cord mesenchymal stem cells reduce fibrosis of bleomycin-induced lung injury. Am J Pathol **175,** 303, 2009.
71. Care, A., Felicetti, F., Meccia, E., *et al*. HOXB7: a key factor for tumor-associated angiogenic switch. Cancer Res **61,** 6532, 2001.
72. Kachgal, S., Mace, K.A., and Boudreau, N.J. The dual roles of homeobox genes in vascularization and wound healing. Cell Adh Migr **6,** 457, 2012.
73. Campagnolo, L., Leahy, A., Chitnis, S., *et al*. EGFL7 is a chemoattractant for endothelial cells and is up-regulated in angiogenesis and arterial injury. Am J Pathol **167,** 275, 2005.
74. Liu, L., Tong, Q., Liu, S., *et al*. ZEB1 upregulates VEGF expression and stimulates angiogenesis in breast cancer. PLoS One **11,** e0148774, 2016.
75. Suleiman, L., Négrier, C., and Boukerche, H. Protein S: a multifunctional anticoagulant vitamin K-dependent protein at the crossroads of coagulation, inflammation, angiogenesis, and cancer. Crit Rev Oncol Hematol **88,** 637, 2013.
76. Tian, Z., Miyata, K., Tazume, H., *et al*. Perivascular adipose tissue-secreted angiopoietin-like protein 2 (Angptl2) accelerates neointimal hyperplasia after endovascular injury. J Mol Cell Cardiol **57,** 1, 2013.
77. Motokawa, I., Endo, M., Terada, K., *et al*. Interstitial pneumonia induced by bleomycin treatment is exacerbated in Angptl2-deficient mice. Am J Physiol Lung Cell Mol Physiol **311,** L704, 2016.
78. Desjardins, M.-P., Thorin-Trescases, N., Sidibé, A., *et al*. Levels of angiopoietin-like-2 are positively associated with aortic stiffness and mortality after kidney transplantation. Am J Hyperten **30,** 409, 2017.
79. Leeper, N.J., Raiesdana, A., Kojima, Y., *et al*. Loss of CDKN2B promotes p53-dependent smooth muscle cell apoptosis and aneurysm formation. Arterioscler Thromb Vasc Biol **33,** e1, 2013.
80. Gross, P.M., Zochodne, D.W., Wainman, D.S., Ho, L.T., Espinosa, F.J., and Weaver, D.F. Intraventricular endothelin-1 uncouples the blood flow: metabolism relationship in periventricular structures of the rat brain: involvement of L-type calcium channels. Neuropeptides **22,** 155, 1992.
81. Zochodne, D.W., Ho, L.T., and Gross, P.M. Acute endoneurial ischemia induced by epineurial endothelin in the

rat sciatic nerve. Am J Physiol Heart Circulat Physiol **263,** H1806, 1992.
82. Tateishi, Y., Osada-Oka, M., Tanaka, M., *et al*. Myeloid HIF-1 attenuates the progression of renal fibrosis in murine obstructive nephropathy. J Pharmacol Sci **127,** 181, 2015.
83. Cho, Y., Shin, J.E., Ewan, E.E., Oh, Y.M., Pita-Thomas, W., and Cavalli, V. Activating injury-responsive genes with hypoxia enhances axon regeneration through neuronal HIF-1α. Neuron **88,** 720, 2015.
84. Frontini, M.J., Nong, Z., Gros, R., *et al*. Fibroblast growth factor 9 delivery during angiogenesis produces durable, vasoresponsive microvessels wrapped by smooth muscle cells. Nat Biotechnol **29,** 421, 2011.
85. Grimmer, C., Balbus, N., Lang, U., *et al*. Regulation of type II collagen synthesis during osteoarthritis by prolyl-4-hydroxylases: possible influence of low oxygen levels. Am J Pathol **169,** 491, 2006.
86. Gilkes, D.M., Bajpai, S., Chaturvedi, P., Wirtz, D., and Semenza, G.L. Hypoxia-inducible factor 1 (HIF-1) promotes extracellular matrix remodeling under hypoxic conditions by inducing P4HA1, P4HA2, and PLOD2 expression in fibroblasts. J Biol Chem **288,** 10819, 2013.
87. Zhou, Y., Jin, G., Mi, R., *et al*. Knockdown of P4HA1 inhibits neovascularization via targeting glioma stem cell-endothelial cell transdifferentiation and disrupting vascular basement membrane. Oncotarget **8,** 35877, 2017.
88. Hinder, L.M., Figueroa-Romero, C., Pacut, C., *et al*. Long-chain acyl coenzyme A synthetase 1 overexpression in primary cultured Schwann cells prevents long chain fatty acid-induced oxidative stress and mitochondrial dysfunction. Antioxid Redox Signal **21,** 588, 2014.
89. Maclennan, D.H., Rice, W.J., and Odermatt, A. Structure/function analysis of the Ca2+ binding and translocation domain of SERCA1 and the role in brody disease of the ATP2A1 gene encoding SERCA1a. Ann N Y Acad Sci **834,** 175, 1997.
90. Hiranandani, N., Bupha-Intr, T., and Janssen, P.M.L. SERCA overexpression reduces hydroxyl radical injury in murine myocardium. Am J Physiol Heart Circ Physiol **291,** H3130, 2006.
91. Rupp, F., Ozcelik, T., Linial, M., Peterson, K., Francke, U., and Scheller, R. Structure and chromosomal localization of the mammalian agrin gene. J Neurosci **12b**, 3535, 1992.
92. Stuart, H.M., Roberts, N.A., Hilton, E.N., *et al*. Urinary tract effects of HPSE2 mutations. J Am Soc Nephrol **26,** 797, 2015.
93. Tamai, S.-i., Imaizumi, K., Kurabayashi, N., *et al*. Neuroprotective role of the basic leucine zipper transcription factor NFIL3 in models of amyotrophic lateral sclerosis. J Biol Chem **289,** 1629, 2014.
94. Cao, W., Lee, S.H., and Lu, J. CD83 is preformed inside monocytes, macrophages and dendritic cells, but it is only stably expressed on activated dendritic cells. Biochem J **385,** 85, 2005.
95. Siebert, J.R., Middleton, F.A., and Stelzner, D.J. Long descending cervical propriospinal neurons differ from thoracic propriospinal neurons in response to low thoracic spinal injury. BMC Neurosci **11,** 148, 2010.
96. van der Wijst, J., Glaudemans, B., Venselaar, H., *et al*. Functional analysis of the Kv1.1 N255D mutation associated with autosomal dominant hypomagnesemia. J Biol Chem **285,** 171, 2010.
97. Imbrici, P., D'Adamo, M.C., Kullmann, D.M., and Pessia, M. Episodic ataxia type 1 mutations in the KCNA1 gene impair the fast inactivation properties of the human potassium channels Kv1.4-1.1/Kvbeta1.1 and Kv1.4-1.1/Kvbeta1.2. Eur J Neurosci **24,** 3073, 2006.
98. Pang, Y., Dong, J., and Thomas, P. Characterization, neurosteroid binding and brain distribution of human membrane progesterone receptors delta and {epsilon} (mPRdelta and mPR{epsilon}) and mPRdelta involvement in neurosteroid inhibition of apoptosis. Endocrinology **154,** 283, 2013.
99. Hou, W., Tian, Q., Steuerwald, N.M., Schrum, L.W., and Bonkovsky, H.L. The let-7 microRNA enhances heme oxygenase-1 by suppressing Bach1 and attenuates oxidant injury in human hepatocytes. Biochim Biophys Acta **1819,** 1113, 2012.
100. Vatner, S.F., Pachon, R.E., and Vatner, D.E. Inhibition of adenylyl cyclase type 5 increases longevity and healthful aging through oxidative stress protection. Oxid Med Cell Longev **2015,** 13, 2015.
101. Hamada, T., Duarte, S., Tsuchihashi, S., Busuttil, R.W., and Coito, A.J. Inducible nitric oxide synthase deficiency impairs matrix metalloproteinase-9 activity and disrupts leukocyte migration in hepatic ischemia/reperfusion injury. Am J Pathol **174,** 2265, 2009.
102. Neilan, T.G., Blake, S.L., Ichinose, F., *et al*. Disruption of nitric oxide synthase 3 protects against the cardiac injury, dysfunction, and mortality induced by doxorubicin. Circulation **116,** 506, 2007.

Address correspondence to:
Adonis Hijaz, MD
University Hospitals Cleveland Medical Center
Urology Institute
11100 Euclid Avenue
Cleveland, OH 44106
USA

E-mail: adonis.hijaz@uhhospitals.org

Received: January 31, 2020
Accepted: May 29, 2020
Online Publication Date: July 2, 2020